Electronic structure of magnetic molecules V_{15}: LSDA+U calculations, x-ray emissions, and photoelectron spectra

D. W. Boukhvalov,[1,2] E. Z. Kurmaev,[2] A. Moewes,[3] D. A. Zatsepin,[2] V. M. Cherkashenko,[2] S. N. Nemnonov,[2] L. D. Finkelstein,[3] Yu. M. Yarmoshenko,[2] M. Neumann,[4] V. V. Dobrovitski,[5] M. I. Katsnelson,[2,6] A. I. Lichtenstein,[7] B. N. Harmon,[5] and P. Kögerler[5]

[1]*Forschungszentrum Jülich, D-52425 Jülich, Germany*

[2]*Institute of Metal Physics, Russian Academy of Sciences Ural Division, Ekaterinburg 620219, Russia*

[3]*Department of Physics and Engineering Physics, University of Saskatchewan, 116 Science Place, Saskatoon, Saskatchewan S7N 5E2, Canada*

[4]*Universität Osnabrück, Fachbereich Physik, D-49069 Osnabrück, Germany*

[5]*Ames Laboratory, Iowa State University, Ames, Iowa 50011*

[6]*Department of Physics, Uppsala University, Box 530, SE-751 21 Uppsala, Sweden*

[7]*University of Nijmegen, NL-6525 ED Nijmegen, The Netherlands*

(Received 30 September 2002; revised manuscript received 16 January 2003; published 8 April 2003)

The electronic structure of magnetic molecules of the type V_{15} (isolated as a cluster compound $K_6[V_{15}As_6O_{42}(H_2O)]\cdot 8H_2O$) has been studied using local spin density approximation (LSDA)+U band structure calculations, and by measurements of x-ray photoelectron (valence band, core levels) and x-ray fluorescence spectra (vanadium $K\beta_5$ and $L_{2,3}$, and oxygen $K\alpha$). Experiments confirm that vanadium ions are tetravalent in V_{15}, and their local atomic structure is close to that of CaV_3O_7. Comparison of experimental data with the results of electronic structure calculations show that the LSDA+U method provides a description of the electronic structure of V_{15} which agrees well with experiments.

DOI: 10.1103/PhysRevB.67.134408 PACS number(s): 75.50.Xx, 75.30.Et, 71.20.−b

I. INTRODUCTION

A new class of magnetic compounds, molecular magnets, has attracted much attention due to unusual magnetic properties that in general are associated with mesoscopic-scale magnetic particles.[1,2] These materials are studied for spin relaxation in nanomagnets, quantum tunneling of magnetization, topological quantum phase interference, quantum coherence, etc.[3–5] In this work, we investigate the polyoxovanadate crystal $K_6[V_{15}As_6O_{42}(H_2O)]\cdot 8H_2O$ (denoted below as V_{15}), in which the cluster anion $[V_{15}As_6O_{42}(H_2O)]^{6-}$ possesses an interesting layered structure.[6–8] This molecule contains 15 antiferromagnetically coupled vanadium ions, each having a spin $S=1/2$; see Fig. 1. In contrast with many other molecular ferrimagnets (such as Mn_{12} or Fe_8), V_{15} is a molecular antiferromagnet with a small net uncompensated spin 1/2, and it exhibits a weak anisotropy. It presents unusual features, such as ''butterfly-like'' hysteresis loops,[9] and, as theoretical estimates suggest,[10] it might exhibit a rather long decoherence time. Previous considerations[6–8,11,12] advocated that vanadium ions in this compound have a valency of 4+. However, experimental studies elucidating the electronic structure of V_{15} are scarce. Such studies are important for theoretical considerations of this complex compound, and firm experimental evidence of the tetravalent nature of vanadium ions in V_{15} is crucial.

We have addressed these issues by investigating V_{15} with x-ray photoelectron (XPS) and x-ray emission (XES) spectroscopies. These techniques allow a determination of the charge (valence) state of the ions, provide information about the total density of states (DOS) normalized to photoionization cross sections and the partial DOS of atomic components in the valence band, indicate variations in chemical bonding character, etc. We present a complete XPS and XES study of valence states of the V ions, and the distribution of the total and partial DOSs in the valence band of V_{15}. The experimental data obtained are compared with theoretical local spin density approximation (LSDA) and LSDA+U calculations, and we show that the results obtained using LSDA+U technique agree well with experiments.

II. SAMPLE PREPARATION AND EXPERIMENTAL DETAILS

The XPS measurements have been carried out with a PHI 5600ci multitechnique spectrometer using monochromatized Al $K\alpha$ radiation ($E_{exc}=1486.6$ eV). The estimated energy resolution is 0.35 eV, and the base pressure in the vacuum

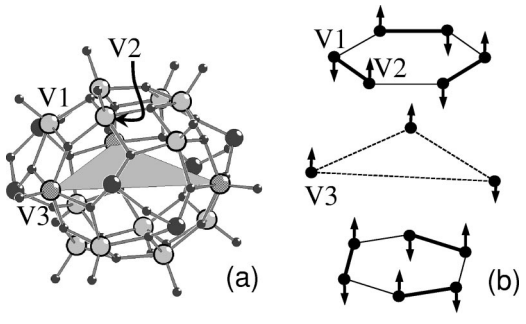

FIG. 1. (a) Structure of the $(K_6[V_{15}As_6O_{42}(H_2O)]^{6-}$ cluster; the large light-gray circles denote the vanadium ions. The central triangle containing the V3 ions is shaded. (b) Schematic sketch of the arrangement of the vanadium ions in V_{15}, and the proposed spin ordering.

chamber during measurements is about 5×10^{-9} Torr.

The XES V $K\beta_5$ spectra ($4p\rightarrow1s$ transition) were measured using a fluorescent Johan-type vacuum spectrometer with a position-sensitive detector.[13] Cu $K\alpha$ x-ray radiation from a sealed x-ray tube has been used for excitation of the V $K\beta_5$ XES. A quartz crystal (rhombohedral plane, second-order reflection) curved to $R=1.8$ m was used as an analyzer. The spectra were measured with an instrumental energy resolution 0.22 eV. The vanadium $L_{2,3}$ ($3d4s\rightarrow2p_{1/2,3/2}$ transitions) and oxygen $K\alpha$ ($2p\rightarrow1s$ transition) XES have been recorded at the Advanced Light Source (Beamline 8.0) employing soft x-ray fluorescence endstation.[14] The vanadium $L_{2,3}$ and oxygen $K\alpha$ XES have been measured resonantly, through the V $L_{2,3}$ and O K edges, and nonresonantly (far from the threshold). The instrumental energy resolutions of the V L and O K spectra are about 0.8 and 0.3 eV, respectively. The V $2p$ and O $1s$ x-ray absorption spectra have been measured in the total electron yield (TEY) mode.

The total resolution of XES measurements is composed of the instrumental resolution (the values given above), and the width of the core level which depends on the lifetime of the hole. For vanadium $K\beta_5$ XES, the width of the core level is about 0.79 eV, which gives about 1.0 eV of total energy resolution. For vanadium L emission, the core level width is about 0.8 eV, and for O $K\alpha$ XES, the core level width is about 0.2–0.3 eV.

The single crystal of $(K_6[V_{15}As_6O_{42}(H_2O)]\cdot8H_2O)$ was prepared as described in Ref. 6. It has a trigonal symmetry (space group $R3c$), as shown in Fig. 1(a). The overall structure consists of three sets of non-equivalent vanadium atoms V1, V2, and V3. V1 and V2 belong to two nonplanar hexagons separated by a triangle of V3 centers forming the ''layer structure'' [Fig. 1(b)].

III. DISCUSSION OF EXPERIMENTAL RESULTS

The x-ray emission valence spectra originate from the electron transitions between the valence band and the core hole. The wave functions of the core states are strongly localized, and the angular momentum symmetry of the core electrons is well defined. Thus, according to the dipole selection rules, these spectra reflect the site-projected and symmetry restricted partial densities of states. However, it is rather difficult to extract information about the occupied V $3d$ states from nonresonant V $L_{2,3}$ XES because V L_3 ($3d4s\rightarrow2p_{3/2}$) and V L_2 ($3d4s\rightarrow2p_{1/2}$) transitions are strongly overlapped due to the small spin-orbit splitting of V $2p$ states (7.7 eV). To overcome this difficulty, we have used resonant excitation of V $L_{2,3}$ XES, where the energy of incoming photons was tuned near V $2p$ thresholds, and in this way we could selectively excite V L_3 XES.

Figure 2 shows the results of measurements of V $L_{2,3}$ XES resonantly excited near the V $2p$ thresholds. The excitation energies were selected in accordance with the features (a–f) on the V $2p$ TEY (upper panel of Fig. 2), and indicated by vertical lines on V L-emission spectra (lower panel of Fig. 2). These energies exactly correspond to the energy of the elastic peaks which probe the unoccupied states, and the

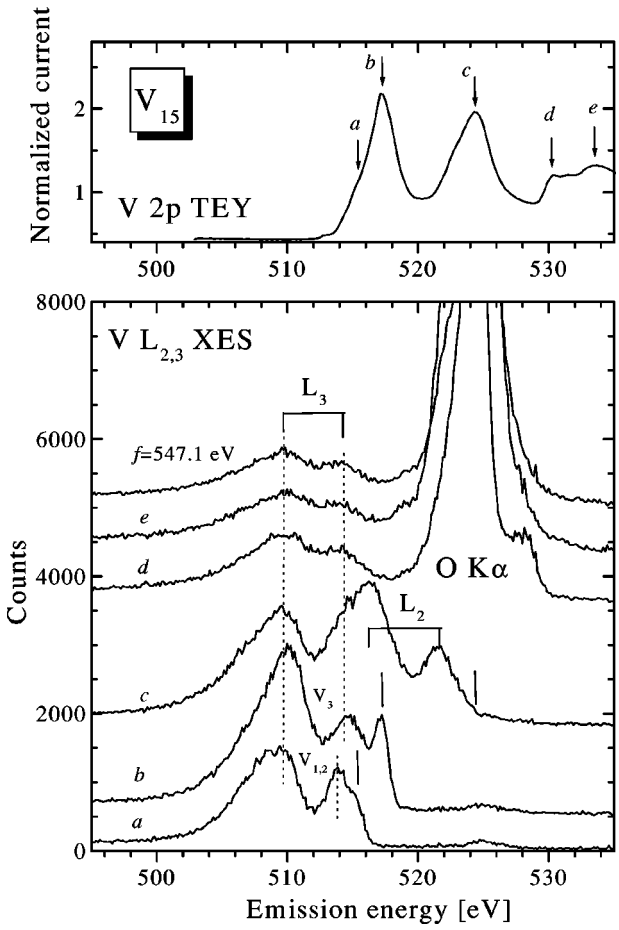

FIG. 2. Excitation energy dependence of V $L_{2,3}$ XES of V_{15}.

resulting intensities follow the absorption cross section. As one can see, the selectively excited V L_3 XES (curves a and b, Fig. 2) reveal two peaks at 510.0 eV and at 513.8–514.4 eV which reproduce the structure of the undistorted distribution of V $3d$ states in the valence band, and can be related to O $2p$ and V $3d$ bands, respectively.[16] The V $3d$-like peaks have different emission energies (513.8 and 514.4 eV), which can be attributed to the contributions of nonequivalent vanadium atoms in the crystal structure of $K_6[V_{15}As_6O_{42}(H_2O)]\cdot8H_2O$ (Fig. 1). The ratio of V $3d$- and O $2p$-(V $3d$)-like peaks is higher for the curve a than for the curve b, which allows us to associate the peak at 513.8 eV with the contributions of V1 and V2 atoms from hexagons (we denote this contribution as 1-2), and the peak at 514.4 eV with the contribution of V3 atoms (we denote this contribution as 3). At higher excitation energies, the peaks at 513.8–514.4 eV are strongly overlapped with the main peak of V L_2 XES (curves c–f, Fig. 2), which makes it very difficult to establish their location and width.

The resonantly excited O $K\alpha$ XES of V_{15} (Fig. 3) reveal significant changes in the fine structure, depending on excitation energy. These changes can be explained by contributions of different oxygens belonging to the polyoxovanadate part and the water of hydration in the V_{15} structure, which are selectively excited by tuning the energy of incoming photons. Using the x-ray fluorescence measurements of liquid

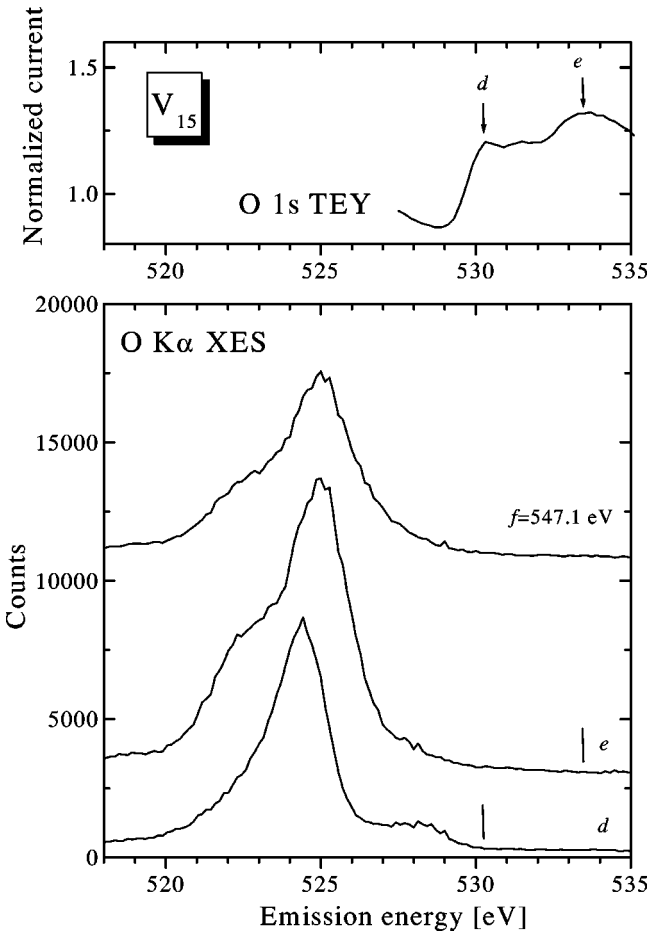

FIG. 3. Excitation energy dependence of O Ka XES of V_{15}.

water,[15] we can attribute the feature e of O 1s TEY (upper panel, Fig. 3) and corresponding O $K\alpha$ XES (curve e, lower panel, Fig. 3) to the oxygens belonging to the water of hydration. We believe that the curve d of O $K\alpha$ XES (lower panel, Fig. 3) corresponds to the contribution of oxygen atoms from the polyoxovanadate part of V_{15}.

In Fig. 4, we compare the XPS valence band and x-ray emission spectra for V $K\beta_5$, V L_3, and O $K\alpha$ XES. To convert the X-ray emission spectra to the binding energy scale, we have used XPS binding energies of core levels (V $2p_{3/2}$, O 1s), emission energy of V $K\alpha_1$ ($2p_{3/2}\rightarrow 1s$ transition), V L_3 ($3d\rightarrow 2p_{3/2}$ transition), and O $K\alpha$ ($2p\rightarrow 1s$ transition) measured for V_{15}. Such a comparison provides a direct interpretation of XPS VB (which probes the total DOS), because the XES of the constituents probe partial DOSs due to the dipolar selection rule. As one can see, at the bottom of the valence band, the O 2s (~22 eV) and K 3p states (~18 eV) are located, as revealed in the XPS VB. V $K\beta_5$ XES also consists of an energy band ($K\beta''$) around 21 eV, because of the hybridization between V 4p and O 2s states. Such a hybridization is typical for all vanadium oxides.[16] According to Fig. 4, in the middle of the valence band V 3d (V 4p) and O 2p states are concentrated, and strong mixing is present. Our spectra demonstrate that at the top of the valence band, the V 3d states prevail.

To analyze the oxidation state of V ions and their local

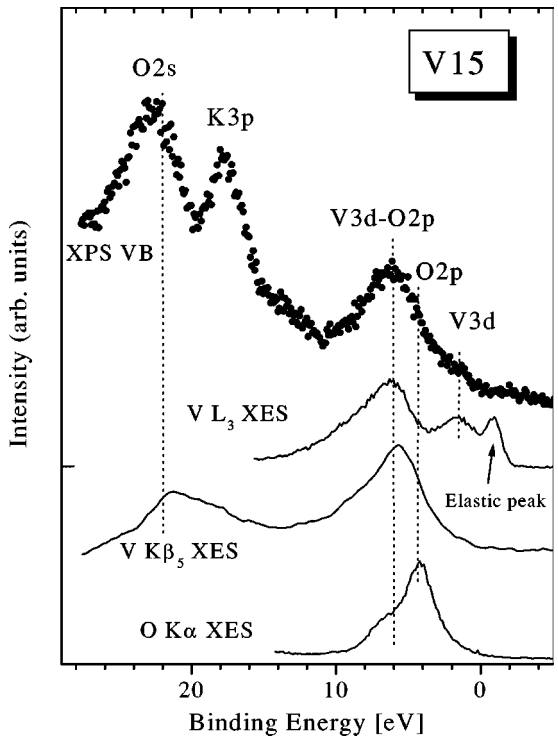

FIG. 4. The comparison of XPS VB and XES of constituents of V_{15} in the binding energy scale.

atomic structure, we have compared V L_3 and V $K\beta_5$ XES of V_{15} with the corresponding spectra of the reference samples VO_2 (where V ions have valency 4+), V_2O_5 (where V ions have a valency of 5+) and CaV_3O_7 (where V ions have a valency of 4+) [Figs. 5(a) and 5(b)]. Figure 5 shows that V $K\beta_5$ and V L_3 XES of V_{15} are closer to those of VO_2 than to V_2O_5, which suggests that vanadium ions are

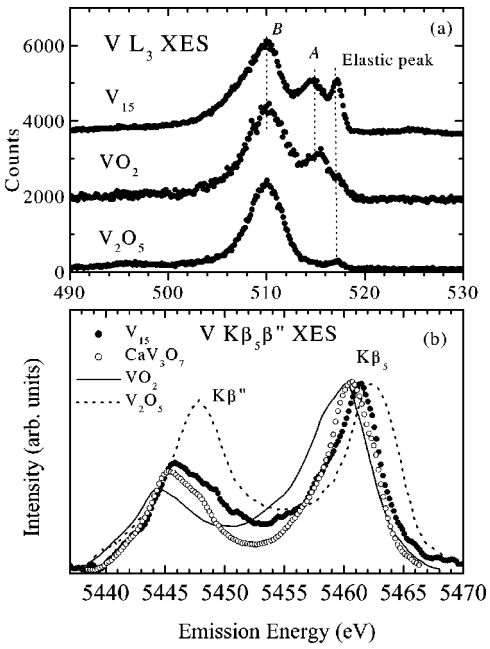

FIG. 5. The comparison of V L_3 (a) and V $K\beta_5$ (b) of V_{15} with spectra of reference samples.

tetravalent in V_{15}. We need to point out that the relative intensity of elastic peak with respect to the main peak of the L spectrum of V_{15} is much higher than that of VO_2 [Fig. 5(a)], although the vanadium ion has the same oxidation state (4+) in both compounds. The elastic peak corresponds to the transitions involving *d* states located above the Fermi level; these states are occupied by a photoelectron in the intermediate state of the absorption-emission process. We can assume that its high intensity indicates that the *d* electrons in V_{15} are more localized as a result of larger V-V distances. Indeed, the average V-V distance in VO_2 is about 2.62 Å, whereas in V_{15} the distance V1-V2 is 2.86 and 3.063 Å.[7] The V3-V3 distances (6.926 Å) in V_{15} are even larger.

It is known that the spectral parameters of V $K\beta_5$ XES (the energy position, the $K\beta''/K\beta_5$ intensity ratio) are very sensitive not only to the oxidation state of V ions in compounds, but also to their nearest neighbors.[16] Therefore, we have chosen CaV_3O_7 (V^{4+} oxidation state) and V_2O_5 (V^{5+} oxidation state) as the reference samples: in these compounds, as well as in V_{15}, vanadium atoms are situated inside a distorted pyramid made by five oxygen atoms.[17,18] A comparison of the V $K\beta_5$ spectra of V_{15}, VO_2, V_2O_5, and CaV_3O_7 [Fig. 5(b)] shows that the energy position, the $K\beta''/K\beta_5$ intensity ratio, and the spectral shape of V_{15} are practically identical to the spectrum of CaV_3O_7, but significantly differ from the V_2O_5 spectrum. This gives experimental confirmation that vanadium ions in V_{15} have the oxidation state (4+) and the configuration of neighboring atoms is similar to that of CaV_3O_7.

IV. SCHEME OF ELECTRONIC STRUCTURE CALCULATIONS

To obtain a deeper understanding of the electronic structure of V_{15}, and to compare the experimental data with theoretical predictions, we have performed a series of LSDA+U calculations.[21] This method is known to provide a good theoretical description for most metal-oxide crystalline systems,[22,23] since in most metal-oxide crystals the account of the on-site Coulomb repulsion (characterized by the value of the parameter *U*) is crucial for a correct description of their properties. Moreover, this method has been successfully applied[25] for the molecular magnet Mn_{12}, where account of the on-site Coulomb repulsion yields the correct value for the gap in the electronic spectrum. Therefore, we expect that the LSDA+U approach should also be successful in describing the electronic structure of V_{15}. As shown below, this is indeed the case.

To start the LDA+U calculations one needs to identify the regions where the atomic characteristics of the electronic states have largely survived (''atomic spheres''). Within these atomic spheres one can expand an electron wave function in terms of a localized orthonormal basis $|inlm\sigma\rangle$ (*i* denotes the site, *n* is the main quantum number, *l* the orbital quantum number, *m* the magnetic number and σ the spin index). The density matrix is defined as

$$n^{\sigma}_{mm'} = -\frac{1}{\pi}\int^{E_F} \mathrm{Im}\, G^{\sigma}_{inlm,inlm'}(E)\,dE, \tag{1}$$

where $G^{\sigma}_{inlm,inlm'}(E) = \langle inlm\sigma|(E-\hat{H})^{-1}|inlm'\sigma\rangle$ are the elements of the Green function matrix in this localized representation (the effective Hamiltonian $\hat{H}$ will be defined later). In terms of the elements of this density matrix $\{n^{\sigma}\}$, the generalized local density approximation (LDA)+U functional[21] has the following form:

$$E^{\mathrm{LDA+U}}[\rho^{\sigma}(\mathbf{r}),\{n^{\sigma}\}] = E^{LSDA}[\rho^{\sigma}(\mathbf{r})] + E^{U}[\{n^{\sigma}\}] - E_{dc}[\{n^{\sigma}\}]. \tag{2}$$

Here $\rho^{\sigma}(\mathbf{r})$ is the charge density for the electrons with the spin σ, and $E^{LSDA}[\rho^{\sigma}(\mathbf{r})]$ is the standard LSDA functional. Equation (2) asserts that the LSDA suffices in the absence of orbital polarizations, which are given by

$$E^{U}[\{n\}] = \frac{1}{2}\sum_{\{m\},\sigma} \langle m,m''|V_{ee}|m',m'''\rangle n^{\sigma}_{mm'} n^{-\sigma}_{m''m'''} + (\langle m,m''|V_{ee}|m',m'''\rangle - \langle m,m''|V_{ee}|m''',m'\rangle) n^{\sigma}_{mm'} n^{\sigma}_{m''m'''}, \tag{3}$$

where V_{ee} is the screened electron-electron interactions. The matrix elements of V_{ee} are defined via an average Coulomb parameter *U* and the Hund intra-atomic exchange constant[21] *J*. Finally, the last term in Eq. (2) describes the correction for the double counting (in the absence of orbital polarizations, Eq. (2) should reduce to E^{LSDA}), and is given by[21]

$$E_{dc}[\{n^{\sigma}\}] = \frac{1}{2}UN(N-1) - \frac{1}{2}J[N^{\uparrow}(N^{\uparrow}-1) + N^{\downarrow}(N^{\downarrow}-1)], \tag{4}$$

where $N^{\sigma} = \mathrm{Tr}(n^{\sigma}_{mm'})$ and $N = N^{\uparrow} + N^{\downarrow}$.

In addition to the usual LDA potential, we determine an effective single-particle potential

$$V^{\sigma}_{mm'} = \sum_{m',m''} \{\langle m,m''|V_{ee}|m',m'''\rangle n^{-\sigma}_{m''m'''} + (\langle m,m''|V_{ee}|m',m'''\rangle - \langle m,m''|V_{ee}|m''',m'\rangle) n^{\sigma}_{m''m'''}\} - U\left(N-\frac{1}{2}\right) + J\left(N^{\sigma}-\frac{1}{2}\right), \tag{5}$$

to be used in the effective single-particle Hamiltonian

$$\hat{H} = \hat{H}_{LSDA} + \sum_{mm'} |inlm\sigma\rangle V^{\sigma}_{mm'} \langle inlm'\sigma|. \tag{6}$$

The linearized muffin-tin orbitals method in the orthogonal approximation has been used for the LSDA calculations.

V. DISCUSSION OF THE RESULTS OF ELECTRONIC STRUCTURE CALCULATIONS

To make the calculations feasible and reasonably precise, we have followed standard practice,[25,26] excluding from consideration the molecules of water of hydration, but retaining

completely the polyoxovanadate part of the V_{15} molecule. The positions of constituent ions have been obtained from the x-ray data. The calculations presented below have been made for $J=0.8$ eV and $U=4$ eV. The choice of appropriate values of U and J for the V_{15} molecule presents a problem. For compounds with small number of atoms in the crystal cell, there are ways of estimating U and J, but for large systems (like V_{15}) such methods are inapplicable due to technical difficulties. Therefore, we choose another approach. First, we note that for the vast majority of compounds with $3d$ elements, the value of J lies between 0.8 and 1.0 eV. In particular, for vanadates, this parameter ranges from 0.81 eV for VO (Ref. 21) to 0.88 eV for CaV_3O_7.[24] The spread of values is very small, and an exact value of J (within the range 0.8–0.9 eV) is of little significance for electronic structure calculations. In contrast, the parameter U is important. For vanadates, the value of U changes from 3.6 eV for CaV_3O_7,[24] to 6.7 eV for VO.[21] Here we choose a value of U close to that of CaV_3O_7, where vanadium ions have the same oxidation state (4+), and a similar configuration of neighboring atoms. Moreover, this value of U gives reasonable agreement with experiment, so that we have reasons to believe that $U=4$ eV is a good estimate for this parameter. We have also checked that the calculations for other values of U, from 3.8 to 5.4 eV, do not significantly change the DOS, but the distance between the bands increases with U.

We note that our calculations with $U=J=0$ (which coincide with the atomic sphere approximation LSDA approach) do not give correct results, exhibiting qualitatively erroneous non-zero DOS at the Fermi level. As reported in Refs. 12 and 27, the use of the LSDA approach with a Gaussian basis and a generalized gradient approximation functional, along with theoretical optimization of the structure of V_{15} molecule, gives a gap between the occupied and nonoccupied states, with zero DOS at the Fermi energy. As can be concluded from Ref. 27, this approach does not agree with some details present in the XES spectra, e.g., the O $2p$ and V $3d$ bands are separated by a larger interval than obtained experimentally, and than given by our LSDA+U calculations with $U=4$ eV. The situation is not yet clear, and further work is needed to clarify the details of the electronic structure of V_{15}; therefore, we do not discuss this issue further here.

The calculated DOS of d, p, and s electrons of inequivalent V1, V2, and V3 ions are presented in Figs. 6–8, and the DOS of oxygen ions belonging to the polyoxovanadate part of the V_{15} molecule are shown in Fig. 9. The total DOS of electrons in the V_{15} molecule is presented in Fig. 10. Until now, detailed quantitative experimental information on the electronic structure of V_{15} has been lacking, but the results of our calculations agree with available qualitative experimental facts. That is, a finite gap ($\Delta E \sim 1$ eV) in the total DOS is correctly reproduced by the LSDA+U calculations. In this work, using the results of XES and XPS investigations described above, we can make quantitative comparison between theory and experiment.

The d electrons of the vanadium ions determine the magnetic behavior of V_{15}. Previous magnetic measurements,[6–8]

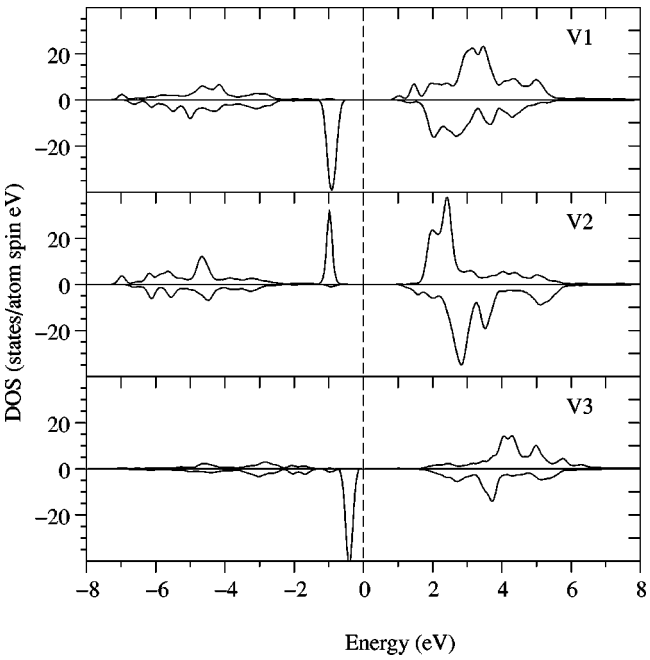

FIG. 6. DOS of d electrons of inequivalent V1, V2, and V3 ions.

and the results of XES/XPS studies presented above, confirmed that V ions are tetravalent, with the total spin 1/2 per ion. Moreover, the measurements of dc spin susceptibility and EPR data suggest that the intra-molecular exchange interactions between V1 and V2 (belonging to the upper and lower hexagons) are strong, while the exchange with V3 ions is much smaller.

These facts agree well with our theoretical results. The calculated $3d$ DOS of all vanadium ions (see Fig. 6) demonstrate two pronounced features: the sharp peaks located at

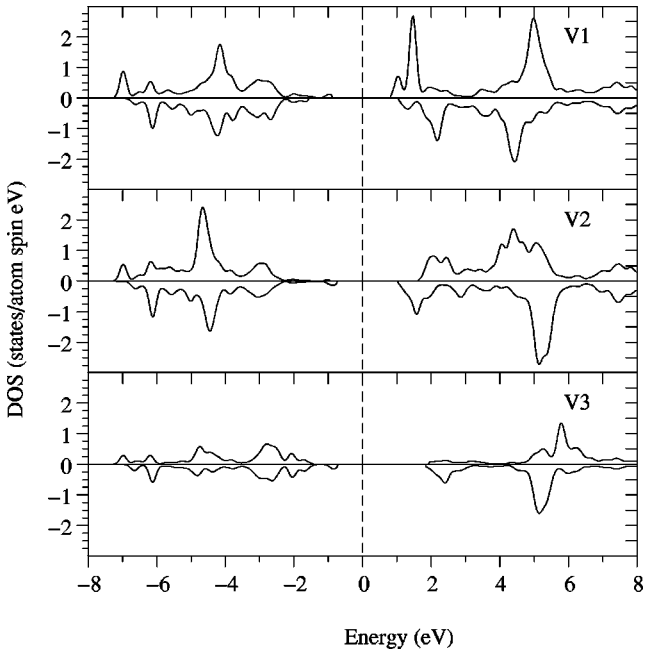

FIG. 7. DOSs of p electrons of inequivalent V1, V2, and V3 ions.

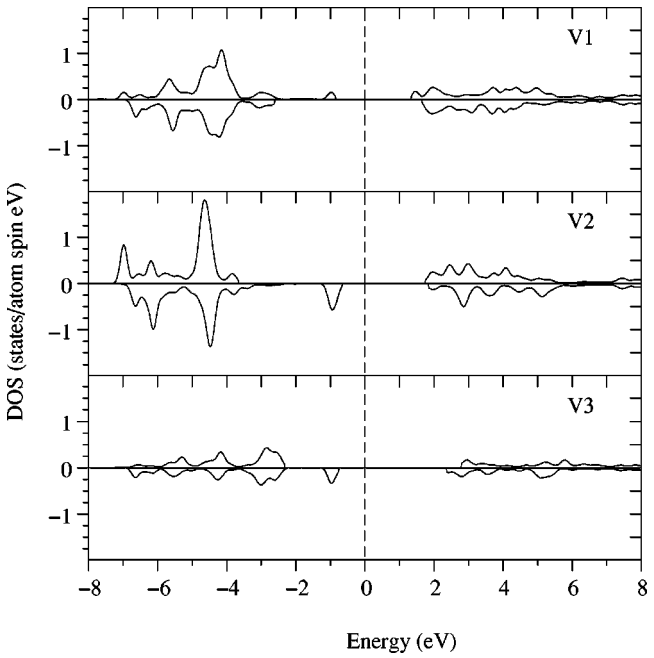

FIG. 8. DOS of *s* electrons of inequivalent V1, V2, and V3 ions.

about -1 eV from the Fermi level for V1 and V2 (for V3, about -0.5 eV), and the broad bands extended between -2 eV and -7 eV. The sharp peaks correspond to localized V *d* electrons associated with the well-defined local spin $S=1/2$ of vanadium ions. Our calculations, indeed, give the values of magnetic moments very close to $1\mu_B$, namely,

$$\mu=-0.94\mu_B \quad \text{for V1},$$

$$\mu=0.91\mu_B \quad \text{for V2},$$

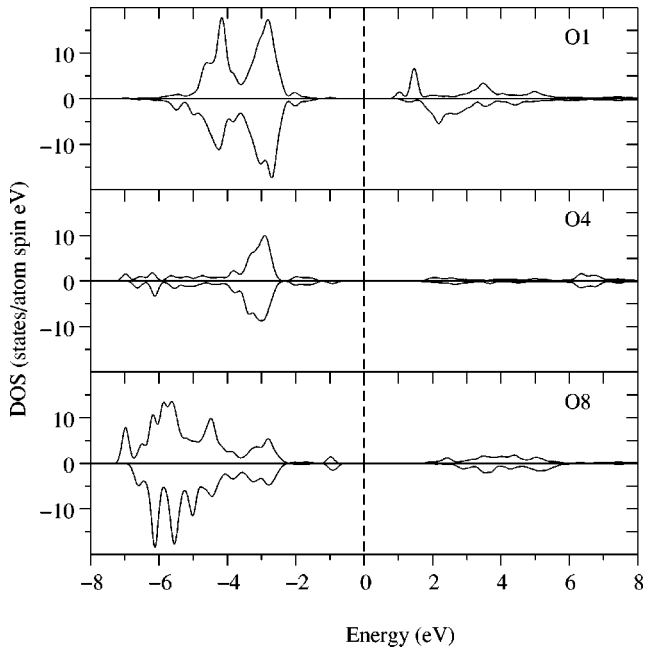

FIG. 9. Total DOSs of *p* electrons of oxygens belonging to the polyoxovanadate part of the V_{15} molecule.

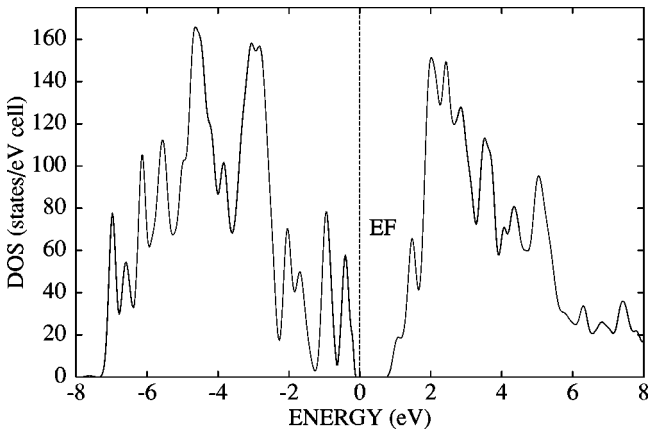

FIG. 10. Total electronic DOS of the polyoxovanadate part of the V_{15} molecule.

$$\mu=-1.0\mu_B \quad \text{for V3}. \tag{7}$$

The charges of V ions have also been calculated from occupancies of $3d$ and $4s$ states of V. The resulting values are very close to $+4$: 4.06 for V1, 4.09 for V2, and 4.00 for V3. The broad bands in the spectrum of V *d* electrons clearly demonstrate the signatures of hybridization between the V *d* and *s* states, on one hand, and the O *p* states, on the other. The broad structure of O *p* DOS is reproduced in V1 and V2 *d* and *s* DOSs and, somewhat weaker, in V3 *d* and *s* DOSs. This is in agreement with the fact that magnetic superexchange interactions between V1 and V2 (located in upper and lower hexagons) are very strong ($\sim$800 K, according to Ref. 7), and involve strong hybridization between V $3d$ and O $2p$ orbitals, while the interactions of V3 (located in the central triangle) are much weaker, implying weaker hybridization. Similar hybridization signatures between V *s* orbitals and O *p* orbitals (see Figs. 8 and 9) correspond to chemical bonding of V with surrounding oxygens.

The calculated DOSs are in agreement with the results of XES measurements. The two features of vanadium DOSs, the sharp peaks and the broad bands, correspond to the two wide peaks, at about -1.5 and -6 eV, clearly seen in the vanadium L_3 XES spectrum in Figs. 2 and 4. In agreement with experimental data, the sharp ''magnetic'' peak in V3 is closer to the Fermi level, than the ''magnetic'' peaks of V1 and V2 (Figs. 2 and 6). The difference between the peak widths and intensities in the calculated DOS and in the measured XES spectra can be attributed to the difference in matrix elements corresponding to different V *d* states. It is known that such a difference can be very large,[28] and it can lead to significant differences between the ''bare'' peak widths or heights in the DOS and the widths/intensities of corresponding peaks as observed in XES spectra. Therefore, following common practice, we have restricted our discussion to the peak positions, rather than widths and heights. Furthermore, the structure of calculated V *p* states DOS is in good agreement with the XES spectra (Figs. 7 and 4). The broad band extending between -2 and -8 eV is revealed in the V $K\beta_5$ XES spectra as a wide peak located in the same

energy interval. Similarly, the calculated DOS for O p states (a broad band from -2 to -8 eV) exhibits itself as a broad feature in the O $K\alpha$ XES spectra in the same energy range; see Figs. 3 and 4.

The x-ray emission is a selective tool which probes only the states allowed by dipolar selection rules, but XPS probes the total density of states. The calculated total DOS (Fig. 10) exhibits a number of peaks and dips. But the XPS spectra apparently lacks a sufficient energy resolution to ''see'' this fine structure, since the resolution of XPS measurements on dielectric crystals, such as V_{15}, is considerably reduced due to the charging effect. We need to point out that the overall width of the XPS VB spectrum (as opposed to the width of individual peaks and dips) given in Fig. 4 is significantly larger than the width of the calculated total DOS (Fig. 10). This difference can be attributed to a rather restricted basis of the wave functions used in calculations, because only the polyoxovanadate part of the V_{15} molecule has been taken into account. As a result, K $3p$ states and As $4s4p$ states seen in the XPS VB are not reproduced in the calculated total DOS. The width of V-$3d$–O-$2p$ hybridized bands as estimated from the XPS VB in the binding energy region of 0–10 eV, is larger than the calculated width of this band. The difference can be attributed to the contribution of As $4p$-states which are located at the bottom of the XPS valence band[19] and are not treated in our LDA+U calculations. The peaks ratio in the XPS VB does not follow to that of the total DOS, because the total DOS is reflected in the XPS VB spectra with an accuracy of the differences of atomic photoionization cross sections.[20] We cannot give a theoretical estimate for this effect because K $3p$, As $4s$, and As $4p$ states are not taken into account in our electronic structure calculations. We also mention that the ''magnetic'' peaks in the V $3d$ states constitute only a small fraction of the total states in V_{15}. Along with the insufficient resolution, other reasons might reduce the intensity of ''magnetic'' peak, e.g., contamination of the surface (XPS, in contrast with XES, is surface-sensitive, and the peak seen in the bulk XES spectra, can be suppressed if the surface is spoiled), or there may be the final state effects which are not considered in the calculations.

VI. SUMMARY

In this work, we have performed an extensive experimental and theoretical investigation of the electronic structure of V_{15} magnetic molecules. Using XPS and XES, we have confirmed that vanadium ions are tetravalent, and their local atomic structure is close to that of CaV_3O_7. We have managed to separate, identify, and study in detail the contributions from inequivalent vanadium ions V1 and V2 (belonging to the upper and lower hexagons), and V3 (located in the triangle sandwiched between the hexagons) to the XES spectra. For theoretical studies, we have employed the LSDA+U approach with $U=4$ eV, yielding theoretical spectra which compare well with the experimental data. Our calculations also confirm the oxidation state $4+$ of vanadium ions in V_{15}. The main features of the calculated DOS correspond to the peaks seen in XES and XPS spectra for V and O ions. The high intensity of the elastic peak of V L_3 XES indicates the existence of localized states of V, which are due to the peculiar crystal structure of V_{15}, where the V-V distances are much larger than the V-X ones. The calculated magnetic moments of V1, V2, and V3 are very close to $1\mu_B$, i.e., to the moment of a free V^{4+} ion, in contrast with other compounds of tetravalent vanadium.

ACKNOWLEDGMENTS

We are grateful to Dr. Arkady Ellern for a high-precision redetermination of the single crystal x-ray structure of the V15 crystals. Funding by the Russian Foundation for Basic Research (Project Nos. 00-15-96575 and 02-02-16674), NATO Collaborative Linkage Grant (PST.CLG.978044), and the Natural Sciences and Engineering Research Council of Canada (NSERC) is gratefully acknowledged. The work was partially supported by the Netherlands Organization for Scientific Research, NWO Project No. 047-008-16. This work was partially carried out at Ames Laboratory, which is operated for the U. S. Department of Energy by Iowa State University under Contract No. W-7405-82, and was supported by the Director of the Office of Science, Office of Basic Energy Research of the U. S. Department of Energy. The electronic structure calculations were made at the Forschungszentrum Jülich.

[1] O. Kahn, *Molecular Magnetism* (VCH, New York, 1993).
[2] D. Gatteschi, A. Caneschi, L. Pardi, and R. Sessoli, Science **265**, 1054 (1994).
[3] *Quantum Tunneling of Magnetization*, Vol. 301 of *NATO Advanced Study Institute, Series E*: *Applied Sciences*, edited by L. Gunther and B. Barbara (Kluwer, Dordrecht, 1995).
[4] J. R. Friedman, M. P. Sarachik, J. Tejada, and R. Ziolo, Phys. Rev. Lett. **76**, 3830 (1996).
[5] L. Thomas, F. Lionti, R. Ballou, D. Gatteschi, R. Sessoli, and B. Barbara, Nature (London) **383**, 145 (1996).
[6] A. Müller and J. Döring, J. Angew. Chem. Int. Ed. Engl. **27**, 1721 (1988).
[7] D. Gatteschi, L. Pardi, A. L. Barra, A. Müller, and J. Döring, Nature (London) **354**, 465 (1991).
[8] A.-L. Barra, D. Gatteschi, L. Pardi, A. Müller, and J. Döring, J. Am. Chem. Soc. **114**, 8509 (1992).
[9] I. Chiorescu, W. Wernsdorfer, A. Müller, H. Bögge, and B. Barbara, Phys. Rev. Lett. **84**, 3454 (2000).
[10] V. V. Dobrovitski, M. I. Katsnelson, and B. N. Harmon, Phys. Rev. Lett. **84**, 3458 (2000).
[11] C. Raghu, I. Rudra, D. Sen, and S. Ramasesha, Phys. Rev. B **64**, 064419 (2001).
[12] J. Kortus, C. S. Hellberg, and M. R. Pederson, Phys. Rev. Lett. **86**, 3400 (2001).
[13] V. E. Dolgih, V. M. Cherkashenko, E. Z. Kurmaev, D. A. Goganov, E. K. Ovchinnikov, and Yu. M. Yarmoshenko, Nucl. Instrum. Methods Phys. Res. A **224**, 117 (1984).
[14] J. J. Jia, T. A. Callcott, J. Yurkas, A. W. Ellis, F. J. Himpsel, M. G.

Samant, J. Stöhr, D. L. Ederer, J. A. Carlisle, E. A. Hudson, L. J. Terminello, D. K. Shuh, and R. C. C. Perera, Rev. Sci. Instrum. **66**, 1394 (1995).

[15] A. Augustsson, J.-H. Guo, and J. Nordgren, MAX-lab Activity Report, p. 152, 2000, Lund, Sweden.

[16] E. Z. Kurmaev, V. M. Cherkashenko, and L. D. Finkestein, *X-ray Emission Spectra of Solids* (Nauka, Moscow, 1988).

[17] H. G. Bachman, F. R. Ahmed, and W. H. Barnes, Z. Kristallogr. **115**, 110 (1961).

[18] J.-C. Bouloux and J. Galy, Acta Crystallogr., Sect. B: Struct. Crystallogr. Cryst. Chem. **29**, 269 (1973).

[19] H. Anno, K. Matsubara, T. Caillat, and J.-P. Fleurial, Phys. Rev. B **62**, 10 737 (2000).

[20] J.-J. Yeh, *Atomic Calculation of Photoionization Cross Section and Asymmetry Parameters* (Gordon and Breach, London, 1993).

[21] V. I. Anisimov, F. Aryasetiawan, and A. I. Lichtenstein, J. Phys.: Condens. Matter **9**, 767 (1997).

[22] I. V. Solovyev and K. Terakura, Phys. Rev. B **58**, 15 496 (1998).

[23] I. A. Nekrasov, M. A. Korotin, and V. I. Anisimov, cond-mat/0009107 (unpublished).

[24] M. A. Korotin, I. S. Elfimov, V. I. Anisimov, M. Troyer, and D. I. Khomskii, Phys. Rev. Lett. **83**, 1387 (1999).

[25] D. W. Boukhvalov, A. I. Lichtenstein, V. V. Dobrovitski, M. I. Katsnelson, B. N. Harmon, V. V. Mazurenko, and V. I. Anisimov, Phys. Rev. B **65**, 184435 (2002).

[26] Z. Zeng, D. Guenzburger, and D. E. Ellis, Phys. Rev. B **59**, 6927 (1999).

[27] J. Kortus, M. R. Pederson, C. S. Hellberg, and S. N. Khanna, Eur. Phys. J. D **16**, 177 (2001).

[28] V. V. Nemoshkalenko and V. G. Aleshin, *Electron Spectroscopy of Crystals* (Plenum Press, New York, 1979).